J Mol Model (2012) 18:2589–2597
DOI 10.1007/s00894-011-1287-x

ORIGINAL PAPER

Molecular dynamics simulation studies of betulinic acid with human serum albumin

Chandramouli Malleda · Navjeet Ahalawat · Mahesh Gokara · Rajagopal Subramanyam

Received: 8 July 2011 / Accepted: 18 October 2011 / Published online: 11 November 2011

Abstract Betulinic acid (BA) is a naturally occurring pentacyclictriterpenoid possessing anti-retroviral, anti-cancer, and anti-inflammatory properties. Here, we studied the interaction of BA with human serum albumin (HSA) by using molecular docking, and molecular dynamic simulation methods. Molecular docking studies revealed that BA can bind in the large hydrophobic cavity of drug binding site I of sub-domain IIA and IIB, mainly by the hydrophobic interactions and also by hydrogen bond interactions. In which several cyclohexyl groups of BA are interacting with Phe (206), Arg(209), Ala(210), Ala(213), Leu(327), Gly(328), Leu(331), Ala(350), and Lys(351), residues of sub-domain IIA and IIB of HSA by hydrophobic interactions. Also, hydrogen bond interactions were observed between the hydroxyl (OH) group of BA with Phe(206) and Glu(354) of HSA, with hydrogen bond distances of 0.24 nm,0.28 nm respectively. Further, specifically, the molecular dynamics study makes an important contribution in understanding the effect of the binding of BA on conformational changes of HSA and the stability of the protein-drug complex system in aqueous solution. The root mean square deviation values of atoms in the free HSA molecule were calculated from 3000 ps to 5000 ps trajectory and the results were obtained as 0.72± 0.036 nm and 0.81±0.032 nm for free HSA and HSA-BA, respectively. The radius of gyration (*Rg*) values of both unliganded HSA and HSA-BA were stabilized at 2.59± 0.03 nm, 2.51±0.01 nm, respectively. Thus, this work may play an important role in the design of new BA inspired drugs with desired HSA binding affinity.

Keywords Betulinic acid · Docking · Human serum albumin · Molecular dynamics

Chandramouli Malleda and Navjeet Ahalawat contributed equally.

C. Malleda · N. Ahalawat · M. Gokara
Department of Biochemistry, University of Hyderabad, Hyderabad 500046, India

N. Ahalawat
Department of Biotechnology, University of Hyderabad, Hyderabad 500046, India

R. Subramanyam (✉)
Department of Plant Sciences, School of Life Sciences, University of Hyderabad, Hyderabad 500046, India
e-mail: srgsl@uohyd.ernet.in

Introduction

Natural compounds to treat various types of diseases have recently attracted considerable interest due to their versatile biological properties and usually broad safety window during administration. One such group of compounds is triterpenes with betulinic acid. Betulinic acid (BA) is a naturally occurring pentacyclictriterpenoid. The molecular mass of BA is 456.7 Da and its molecular formula is $C_{30}H_{48}O_3$ (See Fig. 1). BA and its derivatives are anti-retroviral, anti-malarial, and anti-inflammatory agents that are not steroids [1–6]. Initially BA was considered to be melanoma specific (undergoing phase II clinical trials) [6] but recent studies suggested that it shows anticancer activity against a broad spectrum of cancers. Anticancer activity has been linked to its ability to directly trigger mitochondrial membrane permeabilization, a central event in the apoptotic process that seals the cell's fate [7]. They were used primarily in the treatment of chronic arthritic conditions and certain soft tissue disorders associated with pain and inflammation. They act by blocking the synthesis of prostaglandins by inhibiting cyclooxygenase, which converts arachidonic acid to cyclic endoperoxides, precursors of prostaglandins. Inhibition of

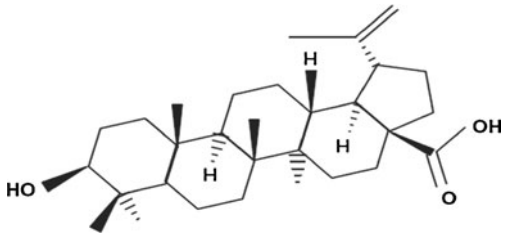

Fig. 1 Structure of betulinic acid

prostaglandin synthesis accounts for their analgesic, antipyretic, and platelet-inhibitory actions [1]. It has been shown that BA suppresses the activity of DNAtopoisomerase I [4]. In addition, molecular modeling experiments have predicted that BA may be a substrate for cytochrome P450 [8]. In other reports, BA derivatives acylated on the C-3-hydroxyl group inhibited HIV-1 replication by interfering with HIV-1 maturation [9, 10].

Interaction studies of drugs with plasma proteins plays a crucial importance to understand the pharmacodynamics and pharmacokinetics of drugs. Drug binding influences the distribution, excretion, metabolism, and interaction with the target tissues. HSA, the most abundant protein in human plasma (~600 mM), is a 67 kDa monomer containing three homologous helical domains, I (residues 1–195), II (196–383) and III (384–585), each divided into A and B sub-domains and the overall structure is stabilized by 17 disulfide bridges [11–15]. An electron density corresponding to residues 1–4 and residues 583–585 of the HSA molecule is not clearly observed, probably due to conformational flexibility at both termini [16]. Structurally, it is a non-glycosylated single polypeptide heart shaped protein with 67% α-helical content (Fig. 2a and b). It binds various endogenous and exogenous ligands including hormones, fatty acids and foreign molecules such as drugs [11–29]. Recently our group has shown that HSA binds to BA with a binding constant of K_{BA}= $1.685\pm0.01\times10^{6}$ M^{-1} [24]. We have also shown that there are conformational changes in protein due to binding of BA to HSA. Also, it is shown in a recent report from our group on different phytomedicines like maslinic acid, trimethoxyflavone, and coumaroyltyramine, sitosterol, strongly binds to HSA leading to change in protein conformation [25–28].

Molecular dynamics (MD) simulation gives insights into the natural dynamics on different timescales of protein-ligand complexes in solution, and affords thermal averages of molecular properties. There have been several MD

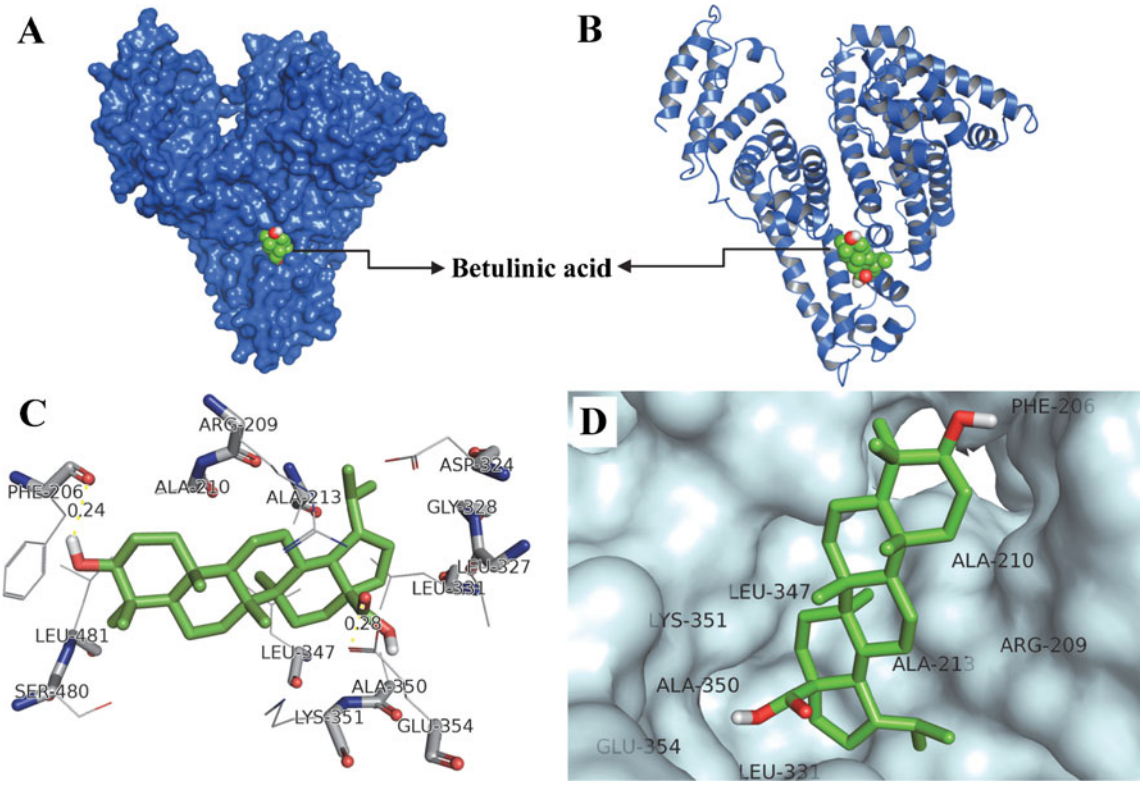

Fig. 2 Betulinic acid docked in the binding pocket of HSA using autodock4.0. Different view of HSA and BA docked conformation, (**a**) overview in surface model of betulinic acid binding to HSA, (**b**) cartoon model, (**c**)The docking poses of the HSA-betulinic acid complex depicted in a ball and stick model (light orange), and HSA, represented the main chain in stick model and side chains in lines model, **d**)Hydrophobic pocket of HSA and betulinic acid, the betulinic acid represents in ball and stick model (orange color) and the binding pockets in cyanocolor, in which the green color represents the binding pocket residues. Images are generated using VMD and PyMol

simulation studies regarding HSA. For example, Sudhamalla et al. [27] studied the stability of HSA-β-sitosterol complex in aqueous solution using MD simulation. Another report by Díaz et al. [30] showed the effect of different protonation states of Lys195 and Lys199 on the IIA binding site using MD simulation. Also Fujiwara and Amisaki [31] performed MD simulations on HSA binding with fatty acids, and their recent work has revealed high and low affinity sites for fatty acids on HSA that are in good agreement with the experimental results [32]. In another report, the HSA–ligand interactions of warfarin and ketoprofen were shown with the molecular dynamic studies which reveal the binding of these ligands to site I and II, respectively [33]. However, a detailed understanding of the interactions between HSA and BA at molecular level has not yet been reported.

In the current study, we used molecular docking to find the binding site and its interactions between HSA and BA at molecular level. Further, MD simulations were performed on HSA–BA complex in aqueous solution to explore the stabilities and dynamic properties of the binding site.

Materials and methods

Molecular modeling and docking

BA docking to HSA was performed with the AutoDock4.0 program using the Lamarckian genetic algorithm [34, 35]. The known crystal structure of HSA (PDB Id: 1AO6) was obtained from the Brookhaven Protein Data Bank. Three dimensional structure of BA was built from its 2D structure, and its geometry was optimized using discover3 in the InsightII/Builder program. Water molecules and ions were removed (including ordered water molecules) and hydrogen atoms added to functional groups with the appropriate geometry within the protein, which was ionized as required at physiological pH. The structure of HSA was protonated in InsightII (www.accelrys.com). Kollman united atom partial charges [36] were assigned to HSA and then non-polar hydrogens of HSA were merged using AutoDock Tools. HSA was held rigid and all the torsional bonds of BA are taken as being free during docking calculations. In docking calculations, the preferred conformation obtained from docking depends on the binding energies of the conformer. Moreover, the protein is usually set to be rigid, and there is no consideration of the effect of solvent molecules on docking. To recognize the binding sites in HSA, blind docking was carried out, the grid size set to 126, 126 and 126 along X-, Y-, and Z-axis with 0.0375 nm grid spacing. The center of the grid set to 2.95, 3.18, 2.35 nm. The docking parameters used were, GA population size: 150; maximum number of energy evolutions: 250,000. During docking, a maximum numbers of top 30 conformers were considered, and the root-mean-square (RMS) cluster tolerance was set to 0.2 nm.

Molecular dynamics simulations

A 5000 ps molecular dynamics simulation of the complex was carried out with GROMACS4.0 [37, 38], package using the GROMOS96 43a1 force field [39, 40]. The initial conformation was taken from the one with binding energy closest to experimental binding energy and binding constant (Table 1). The topology parameters of HSA were created by using Gromacs program. The topology parameters of BA were built by the Dundee PRODRG2.5 server (beta) [41]. Then the complex was immersed in a cubic box (7.335×6.135×8.119 nm) of extended simple point charge (SPC) water molecules [39]. The solvated system was neutralized by adding sodium ions in the simulation box, the entire system was composed of 5843 atoms of HSA, one BA and 15 Na^+ counter ions and 69,491 solvent atoms. To release conflicting contacts, energy minimization was performed using the steepest descent method of 1000 steps, followed by the conjugate gradient method for 1000 steps. MD simulation studies consist of equilibration and production phases. In the first stage of equilibration, the solute (protein, counter ion and betulinic acid) was fixed and the position-restrained dynamics simulation of the system, in which the atom positions of HSA were restrained at 300 K for 30 ps. Finally the full system was subjected to 5000 ps MD at 300 K temperature and 1 bar pressure. The periodic boundary condition was used and the motion equations were integrated by applying the leaf-frog algorithm with a time step of 2 fs. The atomic coordinates were recorded at every 0.5 ps during the simulation for latter analysis. The MD simulation and results analysis were performed on OSCAR Linux cluster with 16 nodes (dual xeon processor) at CMSD facility, University of Hyderabad.

Results and discussion

Our previous *in vitro* report exhibits that BA binding interactions and conformational changes of HSA. From this study the binding constant of BA to HSA was calculated from fluorescence data and found to be $K_{BA}=1.685\pm0.01\times10^6$ M^{-1} [24], indicating a strong binding affinity. It is interesting that the computationally calculated binding constant 1.68×10^6 M^{-1} also accurately matches the experimental value (Table 1). The secondary structure changes that appeared with the HSA–BA complex, indicate that the HSA in this complex is partially unfolded due to binding of BA to HSA.

In principle, there are four types of non-covalent interactions in ligand binding to proteins. Those are hydrogen

Table 1 Docking summary of HSA with betulinic acid by AutoDock program generated different ligand conformers using a Lamarkian genetic algorithm

SN	Rank	Sub rank	Binding energy [kcalM^{-1}]	Inhibitory constant Ki	Ka [M^{-1}]
1	1	1	−10.51	19.76 nM	5.06×10^{7}
2	1	2	−10.42	22.99 nM	4.35×10^{7}
3	2	1	−9.81	64.54 nM	1.55×10^{7}
4	2	2	−9.61	90.61 nM	1.10×10^{7}
5	2	3	−9.6	92.62 nM	1.08×10^{7}
6	3	1	−9.57	96.1 nM	1.04×10^{7}
7	4	1	−9.38	133.15 nM	7.51×10^{6}
8	4	2	−8.98	260.18 nM	3.84×10^{6}
9	5	1	−8.49	594.86 nM	1.68×10^{6}
10	5	2	−8.46	628.55 nM	1.59×10^{6}
11	6	1	−8.19	992.56 nM	1.01×10^{6}
12	7	1	−7.86	1.73 μM	5.78×10^{5}
13	7	2	−7.83	1.81 μM	5.52×10^{5}
14	8	1	−7.83	1.82 μM	5.49×10^{5}
15	8	2	−7.7	2.26 μM	4.42×10^{5}
16	9	1	−7.58	2.76 μM	3.62×10^{5}
17	10	1	−7.58	2.79 μM	3.58×10^{5}
18	11	1	−7.47	3.33 μM	3.00×10^{5}
19	12	1	−7.25	4.84 μM	2.07×10^{5}
20	12	2	−7.19	5.39 μM	1.86×10^{5}
21	12	3	−7.12	6.04 μM	1.66×10^{5}
22	13	1	−7.05	6.76 μM	1.48×10^{5}
23	14	1	−6.94	8.12 μM	1.23×10^{5}
24	14	2	−6.92	8.44 μM	1.18×10^{5}
25	15	1	−6.89	8.97 μM	1.11×10^{5}
26	15	2	−6.84	9.65 μM	1.04×10^{5}
27	15	3	−6.83	9.89 μM	1.01×10^{5}
28	15	4	−6.81	10.27 μM	9.74×10^{4}
29	16	1	−6.67	12.81 μM	7.81×10^{4}
30	17	1	−6.16	30.41 μM	3.29×10^{4}

bonds, van der Waals forces, hydrophobic and electrostatic interactions. The thermodynamic parameters of the interaction are the main evidence for confirming the forces involved. By using the above binding constant, $K_{BA}=1.685\pm0.01\times10^{6}$ M^{-1}, if we calculate the standard free energy according to Eq. 1.

$$\Delta G^{0} = -RT \ln K, \quad (1)$$

where ΔG is free energy, K is binding constant at the corresponding temperature (25 °C) which can be obtained from fluorescence data and R is the gas constant. Thus, the free energy change is−8.5 kcal M^{-1} at 25 °C. These results were fully supported by computational calculation which was obtained as−8.49 kcal M^{-1} (Table 1). A similar type of interaction like hydrophobic and hydrogen bonding were observed with our recent studies of natural compounds, feruloylmaslinic acid, trimethoxy flavones, coumaroyltyramine and β-sitosterol with HSA having binding constants of K_{FMA}1.42 ±0.01×10^{8} M^{-1},K_{TMF}1.0±0.01×10^{3} M^{-1}, and K_{CT} 4.5±0.01×10^{5} M^{-1}, $K_{sitosterol}$4.6 ±0.01×10^{3} M^{-1} and their free energies are −10.9, -5.4, -7.6, and −5.0 kcal, M^{-1} [25–28]. Further, we performed computational studies like molecular docking and simulations to understand more details of its binding and also stable conformation of protein.

Molecular docking studies

Crystal structure analysis has revealed that HSA consists of a single polypeptide chain of 585 amino acid residues and comprises three structurally homologous domains (I–III): I (residues 1–195), II (196–383), and III (384–585) that assemble to form a heart-shaped molecule [17]. The principal regions of ligand binding sites of HSA are located in hydrophobic cavities in sub-domains IIA and IIIA, which correspond to site I and site II, respectively, other than this there are eight fatty acid binding sites [11–13, 23, 42].

In this study, AutoDock program was chosen to examine the binding mode of BA at the active site of HSA. A total of 30 different conformations were generated through blind docking. Based on RMS cluster tolerance between structures, these complexes were sorted into clusters, i.e., different clusters with different binding modes with HSA; finally we obtained 17 clusters (data not shown). Judging from the values of mean binding energy and number of structures in the cluster, cluster 1 was found to be the preferred binding site as it had the lowest mean binding energy (−8.49 kcal M^{-1}) (Table 1) and also it is very close to the experimental value (−8.5 kcal M^{-1}) which was published by our group [24] and the binding constant also matches the experimental value (Table 1). After visual inspection we have observed that out of 30 conformations ten conformations were found in II A and IIB sub-domain. Our lowest energy conformation (Fig. 2a and b) is also found to be docked with sub-domain II A and IIB which can be justified with the results shown by Subramanyam et al. [24]. The fluorescence maximum at 362 nm emission increased with increasing concentrations of BA (0.01–0.1 mM) keeping the concentration of HSA (0.025 mM) fixed. It is important to note that the Trp-214 residue of HSA is in close proximity to the sub-domain IIA. The probable cause of this conformational change may be due to allosteric interaction between domains I, II and III. As sub-domain IIA and IIIA are topologically similar, and the only chance for drug binding is in sub-domain IIA and IIB which have been observed from docking results. So we can say on the basis of AutoDock result that the most probable binding site for BA is between sub-domain IIA and IIB (Fig. 2c and d).

The BA molecule moiety was located within the hydrophobic binding pocket and several cyclohexyl groups of BA interact with Phe(206), Arg(209), Ala(210), Ala(213), Leu (327), Gly(328), Leu(331), Ala(350), and Lys(351), etc.

Table 2 Hydrophobic interaction between BA atoms and HSA atoms with distance (nm)

Ligand(BA)	Residue no	Atom no	Residue	Residue no	Atom no	Distance (nm)
LIG	583	C13	LYS	351	CE	0.366
LIG	583	C13	LYS	351	CD	0.318
LIG	583	C29	ALA	350	CB	0.314
LIG	583	C23	ALA	350	CB	0.35
LIG	583	C11	ALA	350	CB	0.327
LIG	583	C04	ALA	350	CB	0.38
LIG	583	C11	LEU	331	CD2	0.327
LIG	583	C10	LEU	331	CD2	0.373
LIG	583	C10	GLY	328	CA	0.372
LIG	583	C10	LEU	327	C	0.368
LIG	583	C27	ALA	213	CB	0.384
LIG	583	C21	ALA	213	CB	0.319
LIG	583	C19	ALA	213	CB	0.378
LIG	583	C15	ALA	213	CB	0.372
LIG	583	C12	ALA	213	CB	0.303
LIG	583	C03	ALA	213	CB	0.333
LIG	583	C01	ALA	213	CB	0.372
LIG	583	C03	ALA	213	CA	0.356
LIG	583	C01	ALA	213	CA	0.337
LIG	583	C14	ALA	210	CB	0.377
LIG	583	C27	ARG	209	CZ	0.373
LIG	583	C25	ARG	209	CZ	0.346
LIG	583	C25	ARG	209	CD	0.351
LIG	583	C27	ARG	209	CG	0.32
LIG	583	C25	ARG	209	CG	0.309
LIG	583	C02	ARG	209	CG	0.38
LIG	583	C05	PHE	206	CE1	0.386
LIG	583	C08	PHE	206	CD1	0.341
LIG	583	C05	PHE	206	CD1	0.344
LIG	583	C08	PHE	206	CB	0.36

residues of sub-domain binding to drug site I of IIA and IIB of HSA by hydrophobic interaction (Table 2) (Fig. 3) generated by ligplot1.0 [43]. Thus it could be concluded that the interaction of BA with HSA is mainly hydrophobic, which is in perfect agreement with the thermodynamic results obtained from fluorescence emission by Subramanyam et al. [24]. Furthermore, there were also a number of specific hydrogen bonds, because several polar residues in the proximity of the ligand play an important role in binding the BA molecule via H-bonds. Hydrogen bonding interactions were observed between the hydroxyl (OH) group of BA and Phe(206) and Glu(354)of HSA, with hydrogen bond distances of 0.24 nm and 0.28 nm, respectively (Fig. 2a). The results suggested that the formation of hydrogen bonds stabilize the BA–HSA complexes. Therefore, the results of molecular docking indicate that the interaction between BA and HSA are dominated by hydrophobic forces, which is in agreement with the fluorescence data of Subramanyam et al. [24].

Analysis of the dynamics trajectories

In order to investigate the stability of the system (protein, ligand, water, ions, etc.) properties were examined by means of RMS deviations (RMSDs) of HSA and BA with respect to the initial structure, root mean square fluctuations (RMSFs) and the radius of gyration (Rg) of protein. In addition, the stability

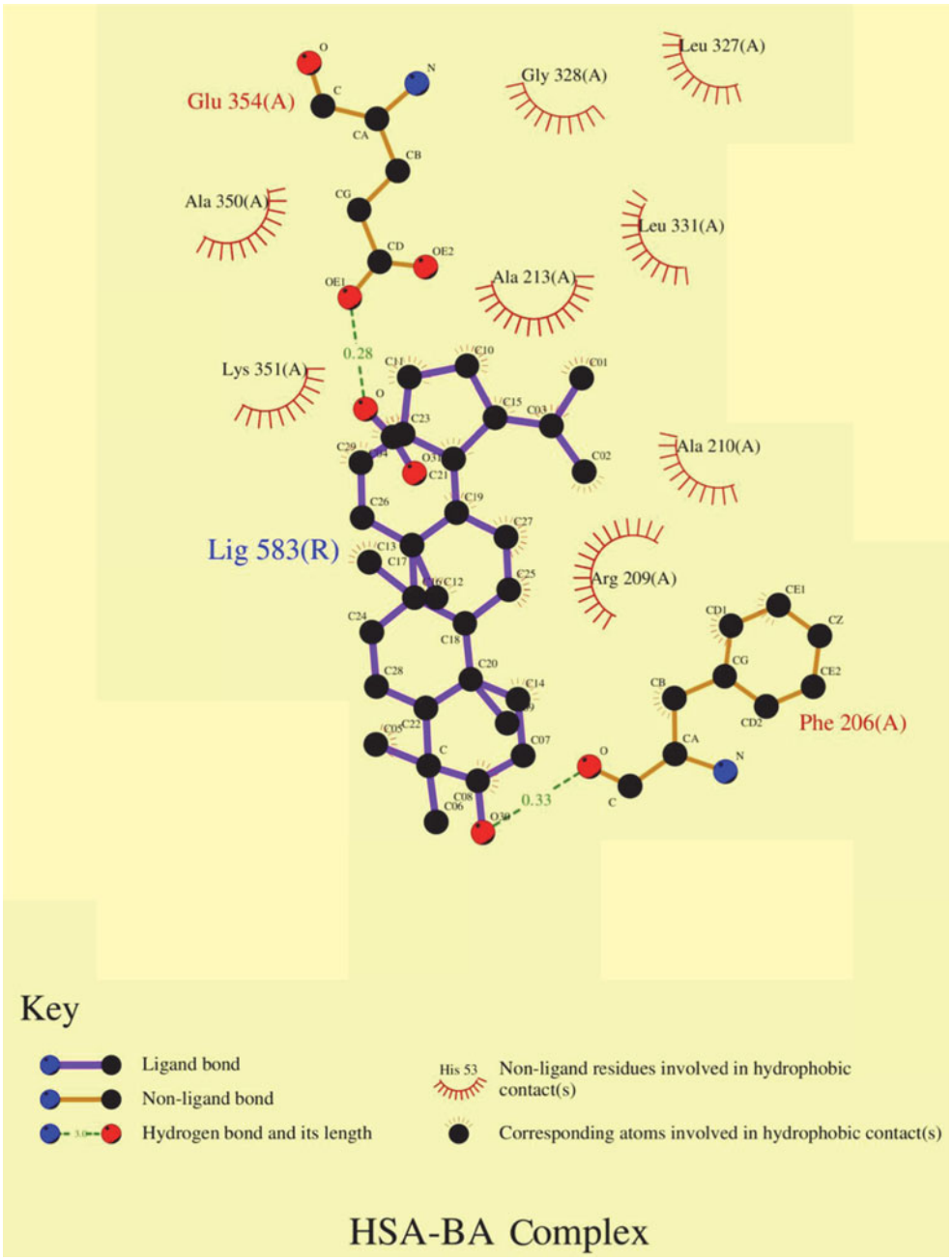

Fig. 3 Representation of betulinic acid interaction with its binding pocket in 2-dimensional view, generated by LIGPLOT 4.5.3

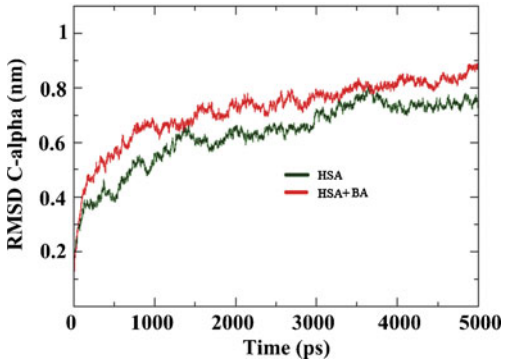

Fig. 4 Time dependence of root mean square deviations (RMSDs). C_α RMSD values for free HSA and HSA- betulinic acid complex during 5000 ps molecular dynamics (MD) simulation

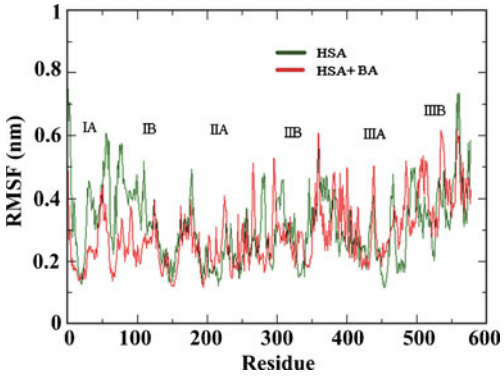

Fig. 6 Root mean square fluctuations (RMSF), time dependence of root mean square deviations (RMSDs). C_α RMSD values for free HSA and HSA-betulinic acid complex during 5000 ps molecular dynamics (MD) simulation

of system proved the credibility of the docking result (Fig. 2), where the BA bound to HSA at drug binding domain IIA and B were used for MD simulations. The RMSD values of atoms in free HSA and HSA-BA with respect to initial structures were calculated along the 5000 ps trajectories and shown in Figs. 4, 5, 6 and 7. Analysis of Fig. 4 indicates that the RMSD of both systems reaches equilibration and oscillate around an average value after 3000 ps simulation time. The RMSD values of atoms for HSA, HSA-BA were calculated from 3000 ps to 5000 ps trajectory data and obtained 0.72± 0.036 nm and 0.81±0.032 nm for free HSA and HSA-BA, respectively. RMSD value of BA binding sub-domain between IIA and IIB of drug binding site 1 (Fig. 4) shows very little deviation in comparison with the whole protein. RMSD of HSA-BA is stabilized at 1000 ps while RMSD of HSA is not stabilized at BA binding site suggesting that the sub-domain IIA and IIB is more favorable for BA binding. After comparing the RMSD of BA binding site and whole protein, it can be stated that binding of BA between sub-domains IIA and IIB leads to the allosteric effect on these domains which was observed by our group by fluorescence analysis [24]. Our group previously reported that the fluorescence emission is increased upon BA binding to HSA, which indicates that binding to the betulinic acid is not close to the tryptophan residue (Trp 214).

In the present MD studies, we determined the radius of gyration (Rg) values of free HSA and HSA-BA complex as shown in Fig. 5. In both systems, Rg values were stabilized at about 3500 ps, indicating that the MD simulation achieved equilibrium after 3500 ps. Initially the Rg values of both free HSA and HSA-BA complex was 2.7 nm. The free HSA, HSA-BA were stabilized at 2.59±0.03 nm, 2.51±0.01 nm, respectively (Fig. 5). The radius gyration of both HSA and HSA-BA are approximately similar to each other which clearly indicate that there are moderate conformational changes during the simulation. Our results clearly match the experimental evidence that the protein conformational changes are marginal while BA is binding to the HSA [24]. Also the previous reports show that during MD simulation conformational changes may occur upon binding of ligands [27, 31–33, 44].

Local protein mobility was analyzed by calculating the time-averaged root mean square fluctuation (RMSF) values of free HSA and HSA-BA complexes were plotted against residue numbers based on the 5000 ps trajectory data (Fig. 6). The general profiles of atomic fluctuations were

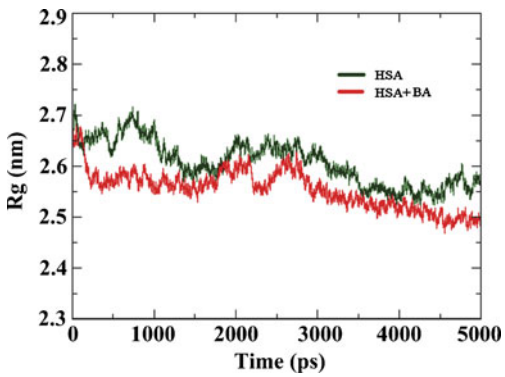

Fig. 5 Time evolution of the radius of gyration (Rg) during 5000 ps MD simulation of HSA and betulinic acid

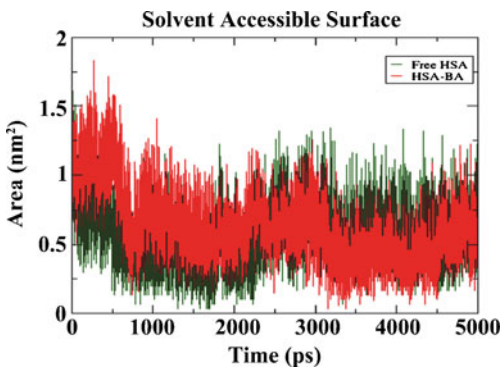

Fig. 7 Graphical representation of the sequence of conformational changes during MD simulation

found to be very similar to each other. Comparison of RMSF for free HSA and HSA-BA in sub-domains IIA and IIB, where BA is binding, shows that RMSF values of HSA-BA was much less than free HSA (Fig. 6), with very little fluctuation.

The solvent-accessible surface area (SASA) defines the surface area of a group that is accessible to a solvent probe. The SASA values for tryptophan residue (Trp214) during this MD simulation were calculated in order to know the effect of BA on sub-domain IIA (drug site I). The SASA value for Trp214 in free HSA has a lower value in comparison with Trp214 in HSA-BA (Fig. 7) which clearly indicates that tryptophan in HSA-BA is more exposed to water than in free HSA. These results are clearly in justification to the fluorescence results shown by Subramanyam et al. [24] that fluorescence emission intensity was increased after complexation of BA with HSA.

Conclusions

Here we have reported betulinic acid binding and conformational changes of human serum albumin by using molecular docking and dynamics simulations. Our previous experimental data [24] is in full agreement with the present computational calculations of free energy which was −8.49 kcal M^{-1}. Nonetheless, BA was bound to HSA mainly by hydrogen and hydrophobic interactions with drug site I at IIA and IIB domain. MD simulation studies revealed that HSA and HSA-BA complexes were stabilized around 3500 ps and also exhibited minor conformational change. The molecular docking, and MD simulation study described herein is a promising approach for probing the interactions of plant medicines with relevant target proteins. Accurate measurements of betulinic acid-albumin binding properties and knowledge of its binding site locations are important to prevent adverse drug reactions and thus this study may help in designing accurate drugs for life-threatening diseases such as cancer, HIV, and so forth.

Acknowledgments We thank Centre for Modelling Simulation and Design, Department of Science and Technology (DST) and DST-Fund for Improvement of Science and Technology for computational facilities at University of Hyderabad, respectively. CM and MG acknowledge University of Hyderabad for Ph.D fellowship.

References

1. Yogeeswari P, Sriram D (2005) Betulinic acid and its derivatives: a review on their biological properties. Curr Med Chem 12:657–666
2. Pisha E, Chai H, Lee IS, Chagwedera TE, Farnsworth NR, Cordell GA, Beecher CWW, Fong HHS, Kinghorn AD, Brown DM, Wani MC, Wall ME, Hieken TJ, Das Gupta TK, Pezzuto JM (1995) Discovery of betulinic acid as a selective inhibitor of human melanoma that functions by induction of apoptosis. Nat Med 1:1046–1051
3. Cichewicz RH, Kouzi SA (2004) Chemistry, biological activity, and chemotherapeutic potential of betulinic acid for the prevention and treatment of cancer and HIV infection. Med Res Rev 24:90–114
4. Chowdhury AR, Mittra N, Sharma S, Mukhopadhyay S, Majumder HK (2002) Betulinic acid, a potent inhibitor of eukaryotic topoisomerase I: identification of the inhibitory step, the major functional group responsible and development of more potent derivatives. Med Sci Monitor 8:254–265
5. Ganguly A, Das B, Roy A, Sen N, Dasgupta SB, Mukhopadhayay S, Majumder HK (2007) Betulinic acid, a catalytic inhibitor of topoisomerase i, inhibits reactive oxygen species–mediated apoptotic topoisomerase i–dna cleavable complex formation in prostate cancer cells but does not affect the process of cell death. Cancer Res 67:11848–11858
6. Rajendran P, Jaggi M, Singh M, Mukherjee R, Burman A (2008) Pharmacological evaluation of C-3 modified Betulinic acid derivatives with potent anticancer activity. Invest New Drugs 26:25–34
7. Fulda S, Kroemer G (2009) Targeting mitochondrial apoptosis by betulinic acid in human cancers. Drug Discov Today 14:885–890
8. Lewis DFV, Dickins M, Weaver RJ, Eddershaw PJ, Goldfarb PS, Tarbit MH (1998) Molecular modeling of human CYP2C subfamily enzymes CYP2C9 and CYP2C19: rationalization of enzyme specificity and site-directed mutagenesis experiments in the CYP2C subfamily. Xenobiotica 28:235–268
9. Li F, Goila-Gaur R, Salzwedel K, Kilgore NR, Reddick M, Matallana C, Castillo A, Zoumplis D, Martin DE, Orenstein JM, Allaway GP, Freed EO, Wild CT (2003) PA-457: A potent HIV inhibitor that disrupts core condensation by targeting a late step in Gag. Proc Natl Acad Sci U S A 100:13555–13560
10. Zhou J, Xiong Y, Dismuke D, Forshey BM, Lundquist C, Lee KH, Aiken C, Chen CH (2004) Pharmacologic inhibition of HIV-1 replication by a novel mechanism: specific interference with the final step of virion maturation. J Virol 78:922–929
11. Curry S, Mandelkow H, Brick P, Franks N (1998) Crystal structure of human serum albumin complexed with fatty acid reveals an asymmetric distribution of binding sites. Nat Struct Mol Biol 5:827–835
12. Curry S, Brick P, Franks NP (1999) Fatty acid binding to human serum albumin: new insights from crystallographic studies. Biochem Biophys Acta (BBA) 1441:131–140
13. Bhattacharya AA, Grnne T, Curry S (2000) Crystallographic analysis reveals common modes of binding of medium and long-chain fatty acids to human serum albumin. J Mol Biol 303:721–732
14. Petitpas I, Grune T, Bhattacharya AA, Curry S (2001) Crystal structures of human serum albumin complexed with monounsaturated and polyunsaturated fatty acids. J Mol Biol 314:955–960
15. Ghuman J, Zunszain PA, Petitpas I, Bhattacharya AA, Otagiri M, Curry S (2005) Structural basis of the drug-binding specificity of human serum albumin. J Mol Biol 353:38–52
16. Sugio S, Kashima A, Mochizuki S, Noda M, Kobayashi K (1999) Crystal structure of human serum albumin at 2.5 Å resolution. Protein Eng 12:439–446
17. He XM, Carter DC (1992) Atomic structure and chemistry of human serum albumin. Nature 358:209–215
18. Chuang VTG, Otagiri M (2001) Flunitrazepam, a 7-nitro-1,4-benzodiazepine that is unable to bind to the indole-benzodiazepine site of human serum albumin. Biochim Biophys Acta 1546:337–345
19. Beauchemin R, N'Soukpo KCN, Thomas TJ, Thomas T, Carpentier R, Tajmir-Riahi HA (2007) Polyamine analogues bind human serum albumin. Biomacromolecules 8:3177–3183

20. Kanakis CD, Tarantilis PA, Tajmir-Riahi HA, Polissiou MG (2007) Crocetin, dimethylcrocetin, and safranal bind human serum albumin: stability and antioxidative properties. J Agric Food Chem 55:970–977
21. Charbonneau D, Beauregard M, Tajmir-Riahi HA (2009) Structural analysis of human serum albumin complexes with cationic lipids. J Phys Chem B 113:1777–1784
22. Froehlich E, Mandeville JS, Jennings CJ, Sedaghat-Herati R, Tajmir-Riahi HA (2009) Dendrimers bind human serum albumin. J Phys Chem B 113:6986–6993
23. Varshney AS, Ahmad P, Rehan E, Rehan M, Subbarao N, Khan RH (2010) Ligand binding strategies of human serum albumin: how can the cargo be utilized? Chirality 22:77–87
24. Subramanyam R, Gollapudi A, Bonigala P, Chinnaboina M, Amooru DG (2009) Betulinic acid binding to human serum albumin: a study of protein conformation and binding affinity. J Photochem Photobiol B 94:8–12
25. Subramanyam R, Goud M, Sudhamalla B, Reddeem E, Gollapudi A, Nellaepalli S, Yadavalli V, Chinnaboina M, Amooru DG (2009) Novel binding studies of human serum albumin with trans-feruloyl maslinic acid. J Photochem Photobiol B 95:81–88
26. Gokara M, Sudhamalla B, Amooru DG, Subramanyam R (2010) Molecular interaction studies of trimethoxy flavone with human serum albumin. PLoS One 5:e8834
27. Neelam S, Gokara M, Sudhamalla B, Amooru DG, Subramanyam R (2010) Interaction studies of coumaroyltyramine with human serum albumin and its biological importance. J Phys Chem B 114:3005–3012
28. Sudhamalla B, Gokara M, Ahalawat N, Amooru DG, Subramanyam R (2010) Molecular dynamics simulation and binding studies of β-sitosterol with human serum albumin and its biological relevance. J Phys Chem B 114:9054–9062
29. Bourassa P, Dubeau S, Maharvi GM, Fauq AH, Thomas TJ, Tajmir-Riahi HA (2011) Binding of antitumor tamoxifen and its metabolites 4-hydroxytamoxifen and endoxifen to human serum albumin. Biochimie 93:1089–1101
30. Diaz N, Suarez D, Sordo TSL, Merz KM (2000) Molecular dynamics study of the IIA binding site in human serum albumin: influence of the protonation state of lys195 and lys199. J Med Chem 44:250–260
31. Si F, Amisaki T (2006) Molecular dynamics study of conformational changes in human serum albumin by binding of fatty acids. Proteins 64:730–739
32. Si F, Amisaki T (2008) Identification of high affinity fatty acid binding sites on human serum albumin by MM-PBSA method. Biophys J 94:95–103
33. Deeb O, Rosales-Hernández MC, Gómez-Castro C, Garduño-Juárez R, Correa-Basurto J (2010) Exploration of human serum albumin binding sites by docking and molecular dynamics flexible ligand-protein interactions. Biopolymers 93:161–170
34. Morris GM, Goodsell DS, Huey R, Olson AJ (1996) Distributed automated docking of flexible ligands to proteins: parallel applications of AutoDock 2.4. J Comput Chem 10:293–304
35. Morris GM, Huey R, Lindstrom W, Sanner MF, Belew RK, Goodsell DS, Olson AJ (2009) AutoDock4 and AutoDockTools4: automated docking with selective receptor flexibility. J Comput Chem 30:2785–2791
36. Morris GM, Goodsell DS, Halliday RS, Huey R, Hart WE, Belew RK, Olson AJ (1998) Automated docking using a lamarckian genetic algorithm and an empirical binding free energy function. J Comput Aided Mol Des 19:1639–1662
37. Berendsen HJC, Van der Spoel D, Van Drunen R (1995) GROMACS: A message-passing parallel molecular dynamics implementation. Comput Phys Commun 91:43–56
38. Lindahl E, Hess B, van der Spoel D (2001) GROMACS 3.0: A package for molecular simulation and trajectory analysis. J Mol Model 7:306–317
39. Van Gunsteren W, Billeter SR, Eising AA, Hünenberger P, Krüger P, Mark A, Scott WRP, Tironi I (1996) Biomolecular Simulation: The GROMOS96 manual and user guide
40. Van Gunsteren WF, Daura X, Mark AE (2002) GROMOS Force Field. Encycloped Comput Chem 2:1211–1216
41. Schuttelkopf AW, van Aalten DMF (2004) PRODRG: A tool for high-throughput crystallography of protein-ligand complexes. Acta Crystallogr 60:1355–1363
42. Li D, Ji B, Sun H (2009) Probing the binding of 8-Acetyl-7-hydroxycoumarin to human serum albumin by spectroscopic methods and molecular modeling. Spectrochim Acta A 73:35–40
43. Wallace AC, Laskowski RA, Thornton JM (1995) LIGPLOT: A program to generate schematic diagrams of protein-ligand interactions. Protein Eng 8:127–134
44. Li J, Zhu X, Yang C, Shi R (2010) Characterization of the binding of angiotensin II receptor blockers to human serum albumin using docking and molecular dynamics simulation. J Mol Model 16:789–798